

# PROJECT ADMINISTRATION DATA SHEET

☒ ORIGINAL ☐ REVISION NO. \_\_\_\_\_

Project No. E-21-J11 R5962-AB1 GTRC/GIT DATE 3 /17 /86  
 Project Director: Dr. D.T. Paris School/Inst EE  
 Sponsor: Naval Coastal Systems Center Panama City, Florida 32407

Type Agreement: Delivery Order No. 0011 Under IQC N61331-85-D-0025 (OCA File 93)

Award Period: From 2/27/86 To 5/26/86 (Performance) 5/26/86 (Reports)

Sponsor Amount: This Change Total to Date

Estimated: \$ 22,942.00 \$ 22,942.00

Funded: \$ 22,942.00 \$ 22,942.00

Cost Sharing Amount: \$ \_\_\_\_\_ Cost Sharing No: \_\_\_\_\_

Title: Investigate Near Wake Bubble Distribution and Transport

## ADMINISTRATIVE DATA

### 1) Sponsor Technical Contact:

Dr. Gary KeKelis

Code 4130

Naval Coastal Systems Center

Panama City, Fl 32407-5000

(904) 234-4281

Defense Priority Rating: DO-C9

OCA Contact R. Dennis Farmer X4280

### 2) Sponsor Admin/Contractual Matters:

Mr. G. Daniel Oldre

Office of Naval Research

Resident Representative

206 O'Keefe Building

Georgia Institute of Technology

Atlanta, Ga. 30332-0490 (404) 347-4381

Military Security Classification: UNCLASSIFIED

(or) Company/Industrial Proprietary: N/A

## RESTRICTIONS

See Attached Government Supplemental Information Sheet for Additional Requirements.

Travel: Foreign travel must have prior approval – Contact OCA in each case. Domestic travel requires sponsor approval where total will exceed greater of \$500 or 125% of approved proposal budget category.

Equipment: Title vests with Georgia Tech if less than \$5,000.00 with prior contracting officer approval.

## COMMENTS:

(Subcontracted to the University of Georgia)

## COPIES TO:

Project Director  
 Research Administrative Network  
 Research Property Management  
 Accounting

Procurement/GTRI Supply Services  
 Research Security Services  
Reports Coordinator (OCA)  
 Research Communications (2)

GTRC  
 Library  
 Project File  
 Other Jones/Legal



SPONSOR'S I. D. NO. 02,103,001,86,004

SPONSORED PROJECT TERMINATION/CLOSEOUT SHEETDate 8/14/86Project No. E-21-J11School EEIncludes Subproject No.(s) N/AProject Director(s) D. T. ParisGTRC / ~~XX~~Sponsor Naval Coastal Systems CenterTitle Investigate Near Wake Bubble Distribution and TransportEffective Completion Date: 5/26/86 (Performance) \_\_\_\_\_ (Reports) \_\_\_\_\_

## Grant/Contract Closeout Actions Remaining:

☐ None☒ Final Invoice or Final Fiscal Report☒ Closing Documents☒ Final Report of Inventions Questionnaire sent to P.I.☒ Govt. Property Inventory & Related Certificate☐ Classified Material Certificate☐ Other \_\_\_\_\_

Continues Project No. \_\_\_\_\_ Continued by Project No. \_\_\_\_\_

## COPIES TO:

Project Director  
Research Administrative Network  
Research Property Management  
Accounting  
Procurement/GTRI Supply Services  
Research Security Services  
Reports Coordinator (OCA)  
Legal Services

Library  
GTRC  
Research Communications (2)  
Project File  
Other A. Jones  
I. Newton  
R. Embry



GEORGIA INSTITUTE OF TECHNOLOGY  
SCHOOL OF ELECTRICAL ENGINEERING  
ATLANTA, GEORGIA 30332

TELEPHONE: (404) 894-2961

July 18, 1986

Naval Coastal Systems Center  
Attn: Dr. Gary Kekelis  
Code 4130  
Panama City, FL 32407

SUBJECT: Final Report  
Project Director: Dr. Charles Uzes, University of Georgia  
Contract No. N61331-85-D-0025: D.O. No. 0011  
"Investigate Near Wake Bubble Distribution and Transport"  
Period Covered: 2/27/86 - 5/26/86

The subject report is forwarded in conformance with the contract specifications.

Should you have any questions or comments regarding this report, please contact the project director or the undersigned.

Sincerely,

Cindy Meyer  
Admin. Asst.

CM

# NEAR WAKE BUBBLE DISTRIBUTION AND TRANSPORT

by

C. A. UZES

in fulfillment of statement of work as per  
contract #

E-21-J11-S1

## Abstract

Sea State data on white water coverage and subsurface bubble distributions are extrapolated to obtain an estimate on the subsurface bubble density scales at 100% coverage. The result is validated through notions on results from white water bubble density and bubble surface lifetime measurements and is then related to time average surface ship near wake bubble densities. A connection is then made between time average surface ship near wake densities and ship speed.

An ensemble of continuity equations describing bubble density evolution over distances less than a turbulent length scale is employed in connection with a turbulent spectrum to define a "random walk" description of bubble evolution. A view of bubble evolution being defined as a consequent set of maps leads to a simple computer code flow chart. The procedure is able to handle the large flow and density gradients that can be expected in the near wake region.



## TABLE OF CONTENTS

INTRODUCTION	1
PART I. Near Wake Bubble Distribution	3
A. White Water Characteristics	3
A-1. Motivation	3
A-2. Sea State Considerations	3
A-3. The White Water Distribution	5
B. White Water Growth, Stabilization, and Decay	6
B-1. White Water Data	6
B-2. White Water Air Volume Currents	7
B-3. White Water Bubble Density Estimates	8
C. The Wake Bubble Density Boundary Value Problem	10
C-1. Bubble Density Evolution with the Free Surface	10
C-2. Sea Surface Boundary Value Problem	11
D. White Water and Surface Ship Densities	13
D-1. White Water Description	13
D-2. Wake Subsurface Air Volume Current Density	14
D-3. Wake Bubble Density Estimates	16
PART II. Near Wake Bubble Transport	17
A. Random Walk Transport Model	17
A-1. Motivation	17
A-2. Transport and Flow Characterization	18
A-3. Equations of Motion	18
A-4. Bubble Evolution	19
A-5. Model Input	20
B. Computer Characterization of Model	21
B-1. Program Description	21
B-2. Program Flow Chart	24
CONCLUSION	25
REFERENCES	27
FIGURES	
Figure I Universal White Water Distribution	28
Figure II Bubble Surface Lifetimes	28
Figure III Wake Centered Coordinate System	29
Figure IV Random Walk Data Planes and Transport	29
TABLE White Water Surface Bubble Characteristics	30

## Introduction

The long range goal of ship wake prediction is to be able to describe ship wake sensor response from surface ship class, environmental, and operating parameters. Since ship wake sensors respond either to the presence of wake turbulence and flow characteristics directly or to the presence of contaminants transported by the hydrodynamic wake, the basis for a ship wake description must necessarily involve a thorough understanding of the ship wake hydrodynamics. Indeed, knowledge of the wake bubble distribution and turbulent diffusion at a downstream Initial Data Plane (IDP) has already been seen to lead to the ability to predict the subsequent wake bubble density evolution and acoustic sensor response in the mid and far wake regions in good agreement with available experimental data. The chief remaining difficulty is the characterization of the near wake, which should describe the near wake hydrodynamics and the transport of contaminants, particularly bubbles.

In the past a great deal of wake data has been obtained by acoustic sensing of wake air bubbles and by interpreting the data using hydrodynamic and bubble transport models. But at present there exists no reliably interpretable acoustic data on the near wake. This are two reasons for this. First it is very difficult to get meaningful data so close to a ship's stern and secondly there exists no presently developed routines for interpreting acoustic sensor response associated with scattering and diffraction by bubbles in a region with a large anticipated air volume fraction. Hence one needs another method for

inferring the wake bubble density distribution in the near wake region. The method of approach followed here is to investigate the implications of the existence of the visible white water surface wake, which in a practical sense defines the extent of the near wake region.

In Part I of this report the connection between surface white water and the air bubble densities below is investigated. In the context of a diffusive transport model it is shown that knowledge of the surface bubble distribution below the white water (hereafter referred to as the subsurface distribution) implies the bubble distribution in the wake below, given the flow velocities. Theoretical models for relating sea state to white water coverage<sup>1,2,3</sup> and subsurface bubble distributions<sup>4,5,6</sup> are then reviewed, as is their consistency with experimental measurements. Inferences drawn are then combined with results of visual observations on surface ship white water wake coverage<sup>7</sup> and measurements on bubble surface and whitewater<sup>8,9,10</sup> (patch) lifetimes<sup>11,14</sup> to form estimates on the near wake subsurface bubble densities.

In Part II of this report a description for the transport of the wake bubble population is presented. In the near wake region one expects large density and flow gradients, the presence of which makes use of a diffusive based description of bubble transport inappropriate. The transport mechanism used here is a generalized random walk whose allowed steps are defined by the characteristic trajectories of a set of bubble continuity equations, where each member of the set is in

correspondance to a possible hydrodynamic flow associated with mean and turbulent motion. A detailed formulation of a computer code based upon the external input of hydrodynamic mean flow and turbulent spectrum is included.

## Part I: Near Wake Bubble Distribution

### A. White Water Characteristics

#### A-1. Motivation

Areal and crow's nest photographs of surface ship white water wakes show regions of effectively 100% white water coverage immediately astern a ship, with the coverage decreasing to naught typically 4 to 13 ship lengths downstream depending upon ship length and speed.<sup>7</sup> Experiments with white water foam typically give white water patch lifetimes of approximately 30 seconds, usually much less than the observed white water wake length. Since the breaking wave action producing the white water layer is certainly contained to within a  $1/4$ - $1/2$  ship length astern, it is reasonable to assume that the white water layer is being maintained by a sufficient number of subsurface bubbles rising to the surface. In the present section sea state data is reviewed for the purpose of inferring the subsurface bubble population required to maintain the extent and coverage of the surface ship white water wake.

#### A-2. Sea State Consideration

White water coverage is defined simply as that fraction of the sea surface covered by white water patches. Experimental investigations on white water coverage as a function of sea state have been carried out by Monahan<sup>2</sup> (1971) and Toba and Chaen<sup>3</sup>

(1973) and the results reviewed and analytically analyzed by Wu' (1979). Wu finds that the white water coverage  $W$  is reasonably described by the equation

$$(I-1) \quad W = \alpha U^{3.75}$$

where  $U$  is the wind velocity measured at the standard anemometer height (10 meters above mean sea level). This result comes from an equilibrium consideration, with  $W$  being set proportional to the wind energy flux input to the sea surface, and is in agreement with experimental data.

On the other hand one can also observe that the oceanic bubble population also depends upon wind speed. From the results of Kolovayev and Johnson and Cooke, Wu observes that the total number of bubbles ( $N$ ) per cubic meter at a given depth obeys

$$(I-2) \quad N = \beta U^{4.5}$$

and in addition observes that the oceanic bubble distribution  $\Psi$  giving the number of bubbles per cubic meter per micron is associated with a nearly universal probability density function. That is

$$(I-3) \quad f(x) = \frac{\Psi(x)}{N}$$

is nearly independent of depth and wind velocity, as Figure 1 indicates. In what follows it will be assumed that (I-3)

represents a sea state generated universal white water distribution.

### A-3. The White Water Distribution

The measurements by Kolovayev<sup>5</sup> and Johnson and Cooke<sup>6</sup> give a time average value for the equilibrium subsurface bubble density in a given sea state. As such the subsurface distribution does not represent an equilibrium condition between the white water bubble source current of subsurface bubbles and white water decay through the bursting of bubbles on the white water surface if the white water coverage is less than 100%. Thus if the equilibrium condition between the subsurface bubble population and surface white water is desired it is necessary to extrapolate the experimental data to the case where the white water coverage is 100%.

Using (I-1) one can find the velocity  $U_e$  for which  $W=1$  and then use (I-2) to establish the total number of bubbles at the surface.  $W_u$  gives

$$\alpha = 1.7,$$

while one can infer

$$\beta = 13.92$$

This implies

$$(I-4) \quad U_e = 39.8 \text{ m/s}, \quad N_e = 2.2 \times 10^8 \text{ B/m}^3.$$

The bubble distribution is then set by a proper choice of the distribution function  $f(r)$ , or equivalently  $\psi$  with  $N_e$  given by (I-4). Through trial and error it is found that a

sufficiently close fit to either of the distributions of Kolovayev or Johnson and Cooke is obtained with

$$(I-5) \quad f(r) dr = \frac{x^p [1 - \exp(-1/x^q)] dx}{\int_0^{\infty} x^p [1 - \exp(-1/x^q)] dx}$$

where

$$(I-6) \quad x = r/a ,$$

and where "a" is a characteristic bubble size given below.

## B) White Water Growth, Stabilization, and Decay

### B-1. White Water Data

The data of Table 1 is extracted from Podzimek<sup>11</sup> and illustrates the measured characteristics of bubbles (larger than 300 microns) lying in a white water foam patch. The table gives the average number of bubbles  $\bar{n}$  per unit surface area of the patch, the mean radius  $\bar{r}$ , the average bubble wall thickness  $\theta$ , and the liquid/air volume fraction  $V_l/V_a$  of the patch.

As one can infer from the table, the average bubble size increases with the age of the patch at a rate of about 100 microns every second. This implies that the average initial bubble size in a freshly created patch is of the order of 200 microns, a figure which from the discussion below can be seen to be compatible with the results of the measured sea state distributions.



The reason for the evolutionary behavior of the white water patch surface bubbles can be attributed to the fact that the bubble surface lifetimes of small microbubbles is very short compared to large microbubbles (.01 sec to .3 sec for 50 to 500 microns). One can consider that there is little difference between a small microbubble in contact with either the sea surface or a large microbubble. As the larger bubbles accumulate more air from the smaller they also become more stable, up to a radius of approximately 3000 microns as Figure II shows (where the slope of the lifetime curve starts to decline). This apparent upper limit on radial size in the white water surface bubble population may be tied to this decrease in stability.

## B-2. White Water Air Volume Currents

The rate of change in air volume of the white water patch per unit area is given by

$$(I-7) \quad \frac{1}{A} \frac{dV}{dt} = J_B - J_{ww},$$

where  $J_{ww}$  is the white water air volume current due to bubbles bursting at the air-water interface,  $J_B$  is the air volume input current from the subsurface distribution, and  $A$  is the surface area of the patch. Thus if  $h$  is the thickness of the white water patch,

$$(I-8) \quad \frac{dh}{dt} = J_B - J_{ww}.$$



Again from the data of Podzimek<sup>11</sup> (Table 1) and from measurements of BSL's<sup>8</sup> ( $t_{BSL}$ ) one can estimate the white water air volume current

$$(I-9) \quad J_{WW} \approx \frac{4}{3} \pi \bar{r}^3 \times \frac{\bar{n}}{t_{BSL}(\bar{r})}.$$

From the data we take

$$\bar{r}^2 \approx \bar{r}^3 \approx (.2 \text{ cm})^3, \quad \bar{n} \approx \frac{6B}{\text{cm}^2}, \quad t_{BSL}(\bar{r}) = 4s,$$

leading to

$$(I-10) \quad J_{WW} \approx .05 \frac{\text{cm}^3}{\text{cm}^2 \cdot \text{sec}}.$$

Note that  $J_B$  is given in terms of the distribution function by

$$(I-11) \quad J_B = \frac{4\pi}{3} \int_0^{r_{max}} r^3 v_T(r) \Psi(r) dr,$$

where  $v_T(r)$  is the bubble buoyant terminal velocity.

### B-3 Bubble Density Estimates

On the scale of the approximations discussed, it remains to determine the appropriate values of  $p$  and  $q$  to be used in the subsurface distribution function (I-5). Wu<sup>4</sup> gives the range of values  $5 > q-p > 3.5$  while Podzimek<sup>11</sup> notes that (equivalently)  $q-p = 4.17$  for the larger bubbles of the white water surface distribution. If it is assumed that the white water average

bubble size growth rate of approximately 100 microns/sec is uniform for bubbles larger than say 200 microns then the Podzimek value suggests 4.17 for the subsurface distribution.

Due to limitations on the experimental measurements the appropriate value of  $p$  is not established. Downstream data on wakes suggests that  $p=0$  in contrast to that of Kolovayev<sup>5</sup> and Johnson and Cooke,<sup>6</sup> and this suggestion is also in better agreement with more recent optical (laser) data of Baldy and Bourguel<sup>12</sup> and with the observed decrease in dissolution of small bubbles attributed to contamination. Hence here  $p=0$ .

At some point in the white water wake one must have a stability point defined by

$$(I-12) \quad \left. \frac{dh}{dt} \right|_x = 0$$

where  $x$  here denotes downstream distance along the wake axis. Using (I-3), (I-5), (I-8), and (I-10) and (I-11) one finds that at this point

$$(I-13) \quad N_o = \frac{J_{ww}}{\frac{4}{3}\pi \int r^3 v_r(r) f(r) dr}$$

With

$$a = 100 \text{ microns,}$$

corresponding to a subsurface distribution average value  $\bar{r} \cong 70 \text{ microns}$  (approximately consistent with Kolovayev and

Johnson and Cooke), one obtains

$$(I-14) \quad N_e \approx 5 \times 10^8 B/m^3,$$

in good agreement with (4).

### C. The Wake Bubble Density Boundary Value Problem

#### C-1. Bubble Density Evolution with the Free Surface

Assuming then that the white water loss rate is determined by the white water subsurface distribution and vice-versa, the question arises as to whether knowledge of the subsurface distribution is sufficient to determine the wake bubble density distribution function everywhere below.

Figure III depicts a rectangular coordinate system centered on the stern of a surface ship having the x-axis on the surface pointing downstream and the z axis characterizing depth. Thus the coordinate system moves with the ship speed  $u_s$ . The analysis below involves a steady state description.

The sea surface will be treated here as a free surface, meaning that the mean flow velocity  $w^j$  ( $j=1,2,3$ ) and the effective bubble transport (diffusion) coefficients  $D^j$  satisfy

$$(I-15) \quad w^3(x,y,0) = D^3(x,y,0) = \frac{\partial w^2}{\partial z}(x,y,0) = \frac{\partial w^1}{\partial z}(x,y,0) = 0.$$

The approach below is to show that knowledge of  $\psi(x,y,0;r)$  on the free surface and  $w^j(x,y,z)$  and  $D^j(x,y,z)$  is sufficient to determine the derivatives  $\partial^n \psi(x,y,0)/\partial z^n$  allowing a Taylor series

expansion in  $z$  about  $z=0$  to define  $\psi(x, y, z; r)$  in the wake.

Neglecting bubble coalescence, one can then write a bubble density continuity equation in the form

$$(I-16) \quad \sum_{\alpha} \frac{\partial}{\partial x^{\alpha}} (w^{\alpha} \psi - D^{\alpha} \frac{\partial \psi}{\partial x^{\alpha}}) + (g\psi)_n + \frac{\partial}{\partial z} (w^3 \psi - D^3 \frac{\partial \psi}{\partial z}) = 0,$$

$\alpha = 1, 2.$

## C-2. Sea Surface Boundary Value Problem

Using the binomial expansion

$$(I-17) \quad \frac{\partial^n}{\partial z^n} (fg) = \sum_{s=0}^n \frac{n!}{(n-s)!s!} \frac{\partial^{n-s} f}{\partial z^{n-s}} \frac{\partial^s g}{\partial z^s},$$

simplifying the notation so that  $f_{zn}$  denotes  $\partial^n f / \partial z^n$ , and differentiating (I-16)  $n$  times with respect to  $z$  one obtains

$$(I-18) \quad \begin{aligned} & (n+1) \left\{ D_z^3 \psi_{zn+1} - w_z^3 \psi_n \right\} + \left\{ D_z^3 \psi_{zn+2} - w_z^3 \psi_{zn+1} \right\} \\ &= \sum_{\alpha} \frac{\partial}{\partial x^{\alpha}} \left\{ w^{\alpha} \psi - D^{\alpha} \frac{\partial \psi}{\partial x^{\alpha}} \right\}_{zn} + (g\psi)_{zn} \\ & \quad + \sum_{s=2}^{n+1} \frac{(n+1)!}{(n-s+1)!s!} \left\{ w_z^3 \psi_{zn+1-s} - D_z^3 \psi_{zn+2-s} \right\}. \end{aligned}$$

The second term in brackets on the "lhs" vanishes by virtue of the free surface condition, so that one can see that  $\psi_{zn+1}(x, y, 0; r)$  is given by knowledge of  $\psi, \frac{\partial \psi}{\partial x^{\alpha}}(x, y, 0; r)$ , and  $\frac{\partial^2 \psi}{\partial x^{\alpha} \partial x^{\beta}}(x, y, 0; r)$  and their  $z$  derivatives up to  $n$ th order. Letting  $w_T = w^3(x, y, 0; r)$  denote the bubble buoyant terminal velocity, one finds

$$\begin{aligned}
 \psi_{z^{n+1}}(x, y, 0; r) = & \frac{1}{|W_T| + (n+1) D_z^3} \left\{ \sum_{\alpha} \frac{\partial}{\partial x^{\alpha}} [W^{\alpha} \psi - D^{\alpha} \frac{\partial \psi}{\partial x^{\alpha}}] \right\} \\
 (I-19) \quad & + (q\psi)_{z^n} + \sum_{s=2}^{n+1} \frac{(n+1)!}{(n-s+1)! s!} \times \\
 & \left[ W_{z^s}^3 \psi_{z^{n+1-s}} - D_{z^s}^3 \psi_{z^{n-s+2}} \right] \Big|_{z=0}
 \end{aligned}$$

Since  $\psi_z(x, y, 0; r)$  is given in terms of  $\psi$ ,  $\frac{\partial \psi}{\partial x^{\alpha}}$ ,  $\frac{\partial^2 \psi}{\partial x^{\alpha} \partial x^{\beta}}$  at  $(x, y, 0; r)$ , this is sufficient to show that all the Taylor series expansion coefficients in

$$\begin{aligned}
 \psi(x, y, z; r) = & \psi(x, y, 0; r) + \frac{\partial \psi}{\partial z}(x, y, 0; r) \cdot z \\
 (I-20) \quad & + \frac{1}{2!} \frac{\partial^2 \psi}{\partial z^2}(x, y, 0; r) \cdot z^2 + \dots
 \end{aligned}$$

can be found from knowledge of  $\psi(x, y, 0; r)$ . Thus the wake distribution function is completely determined by the white water subsurface distribution (with the free surface characterization of the sea surface).

Computationally, it is desired to convert the subsurface distribution into one on an initial data plane. The question arises as to how many data points are required on the surface to determine  $\psi$  on the lattice points on the IDP, particularly along the axial direction. Generally speaking computation of the  $n$ th order derivative requires data on  $n+1$  lattice points, or conversely, knowledge of the first  $n$ th derivatives determines the function on  $n+1$  lattice points. Depending upon the model, it is clear that in principle (I-19) can be iterated to obtain the required number of derivatives  $\frac{\partial^{p+q} \psi}{\partial x^{\alpha p} \partial x^{\beta q}}$  along the

surface and thus the number of surface lattice points required.

#### D. White Water and the Surface Ship Bubble Densities

##### D-1. White Water Description

Referring to "Physics of Sound in the Sea", typical white water wakes are illustrated therein in Figures 1-7 of Chapter 26.<sup>13</sup> A common characteristic of the white water wake is a bow wave generated white water trail, a hull boundary layer trail, both followed by and mixing with a trail due to stern wave generated white water to form the initial spreading region (ISR) . Thus one typically has dense region of almost solid white water lasting up to a ship length or so. This dense region then breaks up into patchy white water. The cause of the breakup into a patchy wake is here assumed to be geometrical, the increasing downstream width of the wake causes the solid stream of white water to break up into patches with little loss in white water thickness. Thus it is assumed that the downstream decline in white water thickness is due chiefly to air volume loss.

It is helpful to picture the growth and decay of white water. Measurements on the persistence of bubbles in sea water indicate bubble surface lifetimes (BSL's)  $< .1$  sec for radii  $< 80$  microns and BSLs of 1 sec or longer for bubbles of radii 500 microns or larger.<sup>10</sup> Since the terminal velocity of the very small bubbles is also very small, less than 1 cm/sec, one has the picture of white water foam being first established by larger bubbles rising to and capping the surface and absorbing

the smaller bubbles coming up from below. As the larger bubbles burst they are replenished by the growth of smaller ones as they rise through the white water to the surface.

Measurements on sea foam in the laboratory<sup>14</sup> show a tendency towards a foam thickness of 1.7 cm and an average bubble radius of 2mm, which compares favorably with the white water patch measurements of Podzimek.<sup>14</sup> For taking  $J_g = 0$ , (I-8) implies a foam thickness of

$$(I-21) \quad h = -J_{ww} \times T_L$$

where  $T_L$  is the average lifetime of a white water foam patch at low sea state. Using the data from Table I, where the average white water surface bubble radius  $\bar{r} \approx 2\text{mm}$  while  $T_L \approx 25$  sec, one finds that

$$(I-22) \quad h = 1.25 \text{ cm.},$$

which compares well with the laboratory measurements on foam average foam thickness of 1.7 cm.<sup>14</sup>

#### D-2. Wake Subsurface Air Volume Current

In what follows it will be assumed that at some point near the ships stern (in comparison to the overall white water wake length) the initial white water thickness is roughly independent of the production mechanism. On this basis the time average white water wake subsurface bubble density can be estimated assuming that the white water patch lifetimes are extended by

the subsurface bubble current densities.

Let

$$(I-23) \quad \alpha(t) = \frac{J_B}{J_{WW}}.$$

Then assuming that  $J_{WW}$  is constant, if  $T_W$  denotes the lifetime of the wake beyond the production point the time average value of (I-8) is given by

$$(I-24) \quad \frac{h_W}{T_W} = (\bar{\alpha} - 1) J_{WW},$$

where  $\bar{\alpha}$  is the time average value of  $\alpha(t)$ . Similarly, writing (I-21) in the form

$$(I-25) \quad \frac{h}{T_L} = - J_{WW},$$

one can easily determine by taking the ratio of (I-24) and (I-25) that

$$(I-26) \quad \bar{\alpha} = 1 - T_L/T_W.$$

It is reasonable to assume that the standard production thickness occurs near the end of the ISR. Measurements indicate that the ISR has a typical duration of 4-6 seconds.<sup>7</sup> With this in mind we shall take

$$(I-27) \quad T_W \approx (L_{WW} - L_{ISR})/u_s \approx \frac{L_{WW}}{u_s} - 5 \text{ sec.},$$

where  $L_{WW}$  for a large number of ships is given in appendix C of



the Peltzer report.<sup>7</sup>

Noting that ship classes within the DD, BB, and CV ship types and environmental conditions (which can be significant<sup>14</sup>) were not distinguished in the Peltzer report<sup>7</sup>, the table below gives ranges for values of  $\bar{\alpha}$ ,  $T_w$ , and  $u_s$ .

	$\bar{\alpha}$	$T_w$ (sec)	$u_s$ (ft/sec)
DD's	.28 - .75	35 - 100	38 - 42
BB's	.68 - .81	79 - 131	38
CV's	.40 - .71	42 - 87	25 - 37

The interpretation of  $\bar{\alpha}$  is as follows. The peak in the white water distributions of Kolovayev<sup>5</sup> and Johnson and Cooke<sup>6</sup> is near 80 microns. Over the time period of the white water wake decay bubbles in this neighborhood and near the sea surface shift only a few microns in size, which means that there is little change in the effective bubble air volume current. Thus the small variances in  $\bar{\alpha}$  suggest that the white water subsurface densities of the three classes of ships included in the table may be nearly equal beyond the ISR, considering that the large bubbles have had time to rise out of the wake. The subsurface densities are nearly universal for the larger combatants.

### D-3. Wake Bubble Density Estimates

In order to see what the given distribution means in terms of ship wake bubble densities, note that  $\bar{\alpha} = 1$  implies  $\bar{N}_e \approx 2 \times 10^8$  B/m<sup>3</sup>. This means, using the White Water depth dependence  $\psi \sim z^{-2.6}$  (see Wu<sup>4</sup>), bubble densities of  $10^6$  B/m<sup>3</sup> at 7m depth if one makes a direct analogy with Kolovayev<sup>5</sup> sea state data. If a relatively flat effective wake distribution up to a 250 micron cutoff is assumed, consistent with previous sonar measurements and bubble evolution analysis, this would imply a density of  $10000$  B/m<sup>3</sup>  $\mu$ m. This lies in the ballpark suggested by attenuation and wake scattering strength measurements. With another view, if one estimates the total number of subsurface bubbles at propeller shaft depth by scaling the Kolovayev data and distributes them over the propeller wake one obtains a similar estimate of  $12000$  B/m<sup>3</sup>  $\mu$ m. This is again within the ballpark for wake attenuation and scattering strength measurements.

## Part II: Near Wake Bubble Transport

### A. Random Walk Transport Model

#### A-1. Motivation

At present a diffusion model of wake contaminant transport exists which successfully treats the mean down stream evolution of surface ship bubble wakes. However, in the near wake region where large density gradients exist it is possible for contaminants to be transported diffusively faster than physically realizable, since  $\bar{J}_p = -D \bar{\nabla} \psi$  and the bubble gradient can be very large due to the initial conditions. In addition the diffusion approach does not provide a means for the treatment of

wake fluctuations and thus the subsequent fluctuations generated in wake sensors. For this reason a random walk model is developed to treat wake fluctuations and the presence of large density gradients, similar to the method of Thorpe<sup>15</sup>.

#### A-2 Transport and Flow Characterization

It is assumed that a hydrodynamic wake program exists which provides as output a turbulent spectrum, that is a set of velocities  $\{\vec{v}^{(i)}\}$  corresponding to a set of probabilities  $\{p_i\}$  describing the occurrence of these velocities together with a time scale over which these velocities can be expected to occur. The bubble transport is then generated by this hydrodynamic flow spectrum together with a model for the bubble hydrodynamic flow. The latter is treated here by inputting the bubble buoyant terminal velocity.

With respect to a coordinate system fixed on the ship's stern (illustrated in Figure III) at the waterline with the x-axis pointing downwake along the ship's axis, z giving depth, and y transverse position across the wake, the bubble density at  $(x,y,z)$  is given by

$$(II-1) \quad \psi = \sum p_i \psi^{(i)}$$

where  $\psi^{(i)}$  is the density of bubbles due to the possibility of their transport to  $(x,y,z)$  via the flow field  $\vec{v}^{(i)}$ .

#### A-3. Equations of Motion

The evolution of  $\psi^{(i)}$  along the streamline specified by  $\vec{v}^{(i)}$  is determined by the continuity equation<sup>16</sup>

$$(II-2) \quad \psi_t^{(i)} + (q\psi^{(i)})_r + \vec{\nabla} \cdot \{ \vec{v}^{(i)} \psi^{(i)} \} = 0,$$

where it is assumed that the motion along the streamfield  $v^{(i)}(x,y,z)$  is defined for the time  $T$ . Here  $q$  denotes the bubble radial growth velocity. It will be assumed that in the ships reference frame a steady state situation exists, so that all flow parameters are not explicit functions of time and the first term in (II-2) vanishes.

Besides computation of the average density given by (II-1) the ensemble of evolution equations allow for the determination of average current density

$$(II-3) \quad \vec{J} = \sum_i p_i \vec{v}^{(i)} \psi^{(i)}$$

and, for example, fluctuations such as that for the density

$$(II-4) \quad (\Delta\psi)^2 = \sum_i p_i \{ \psi^{(i)} - \psi \}^2$$

#### A-4. Bubble Evolution.

Since the wake evolves downstream  $x$  will be singled out as an evolution parameter. The density will be assumed to be known along a transverse plane  $x_0$  and propagated by the ensemble to the plane  $x$ . Denoting  $u$ ,  $v$ , and  $w$  as the  $x, y$ , and  $z$  components of  $\vec{v}^{(i)}(x,y,z)$ , the solutions to the continuity equation (II-5) is defined most simply by the set of transformations

$$r = r_0^{(i)} + \int_{x_0}^x q \frac{dx}{u^{(i)}} ,$$

$$(II-5) \quad y = y_0^{(i)} + \int_{x_0}^x v^{(i)} \frac{dx}{u^{(i)}} ,$$

$$z = z_0^{(i)} + \int_{x_0}^x w^{(i)} \frac{dx}{u^{(i)}} ,$$

$$(II-6) \quad \psi^{(i)}(x, y, z; r) = \exp \left\{ - \int_{x_0}^x q_r \frac{dx}{u^{(i)}} \right\} \cdot \psi(x_0^{(i)}, y_0^{(i)}, z_0^{(i)}; r_0^{(i)}) .$$

The trajectories (II-5) map the points  $x_0^{(i)}, y_0^{(i)}, z_0^{(i)}$  into the points  $x, y, z$ : so that Figure IV can be considered as characterizing the transport of bubbles to the transverse plane  $x$ . Note that the ability to map simply from transverse plane to transverse plane depends upon the steady state hypothesis.

#### A-5. Model Input

As stated above, a hydrodynamic code must produce the fluid flow spectrum of velocities and their probabilities and the expected correlation time for which these velocities can be considered to exist. In addition the bubble dynamics must be input along with the input of suitable initial and boundary conditions.

The radial growth velocity  $q(z, r)$  can be taken from the "dirty" bubble model wherein surface contaminants are assumed to produce rigid sphere type boundary conditions.

As previously stated the initial data on some constant  $x$

surface is assumed to be provided by some other means. It remains to clarify the sea surface boundary condition.

Free surface boundary conditions are employed here on the fluid flow velocities. This means that

$$(II-7) \quad \frac{\partial u^{(i)}}{\partial z}(x, y, 0) = \frac{\partial v^{(i)}}{\partial z}(x, y, 0) = 0, \quad w^{(i)}(x, y, 0; z) = w_T.$$

Note that the free surface boundary conditions imply that any bubble striking the free surface is lost from the wake since there is then no trajectory taking a bubble back down into the wake - the bubble terminal velocity is always directed towards the surface. Thus the free surface boundary conditions imply that knowledge of the bubble distribution on the initial data plane, the turbulent spectrum, and the bubble dynamic model (including dissolution) is sufficient to determine bubble wake evolution.

## B. Computer Characterization of the Random Walk Transport

### B-1. Program Description

The three dimensional random walk code will involve the repeated passing of data from one three dimensional lattice space to another, a point in the  $n$ th lattice being denoted by the interger triplet  $(i_n, j_n, k_n)$  corresponding to values of the coordinates  $(x_n, z_n, r_n)$ . Figure IV illustrates the representation of the  $n$ th and  $(n+1)$ th lattice spaces by hyperplanes "normal" to the  $x$  (wake) axis with the horizontal direction in each case

corresponding to the combined  $(y,z)$  directions. The contribution of each of the velocity fields  $\vec{v}^{(i)}(x,y,z;r)$  and  $q(z,r)$  to the bubble transport involves the "passing" of bubbles  $\Psi(y_n, z_n; r_n)$  from some initial point  $(y_n, z_n; r_n)$  in the  $n$ th plane along the  $(\vec{v}^{(i)}, q)$  streamlines to the lattice point  $(i_{n+1}, j_{n+1}, k_{n+1})$  or  $(y_{n+1}, z_{n+1}; r_{n+1})$  in the  $(n+1)$ th lattice space, as Figure IV illustrates.

The program basically involves the following steps for each passage:

1. Input of sufficient data to establish the set of trajectories
2. A map consisting of the determination of each of the  $(y_n, z_n; r_n)$  for each  $(i_{n+1}, j_{n+1}, k_{n+1})$
3. The determination of  $\Psi(y_n, z_n; r_n)$  from knowledge of the  $\Psi(i_n, j_n, k_n)$  at all the lattice points in the  $n$ th hyperplane
4. The scaling of the  $\Psi(y_n, z_n; r_n)$  as per (II-6) into the  $\Psi^{(i)}(i_{n+1}, j_{n+1}, k_{n+1})$  along each trajectory, and
5. The weighted averaging of the  $\Psi^{(i)}(i_{n+1}, j_{n+1}, k_{n+1})$  so obtained from all the velocity fields  $(\vec{v}^{(i)}, q)$  via (II-1).

The steps involve the following considerations.

Step 2 involves integration backward in  $x$  along a trajectory from  $(i_{n+1}, j_{n+1}, k_{n+1})$  to an endpoint  $(y_n, z_n; r_n)$  in the  $n$ th plane. Each such integration requires knowledge of  $\vec{v}^{(i)}(x,y,z;r)$  and  $q(z,r)$  along the trajectory. Thus in step 1. velocity field must be input from a hydrodynamics code and will come in terms of values given along discrete steps in  $x$ . The

random walk time step may in the case of a larger turbulent length scale be large in comparison to  $\Delta x$ , which requires that  $v^{(i)}$  be fit using spline functions or treated as constant along each increment  $\Delta x$ . The  $q(z,r)$  can be explicitly input as functions of  $z$  and  $r$  using the bubble dynamic theory for "dirty" bubbles.

Step 3 requires determination of  $\Psi(y_n, z_n; r_n)$  from knowledge of  $\Psi(i_n, j_n; k_n)$  at the lattice points of the hyperplane. This requires input of a suitable interpolation scheme such as weighting the contribution of each of the nearest neighbor lattice points to  $(y_n, z_n; r_n)$  as some function of the distances from the nearest neighbors.

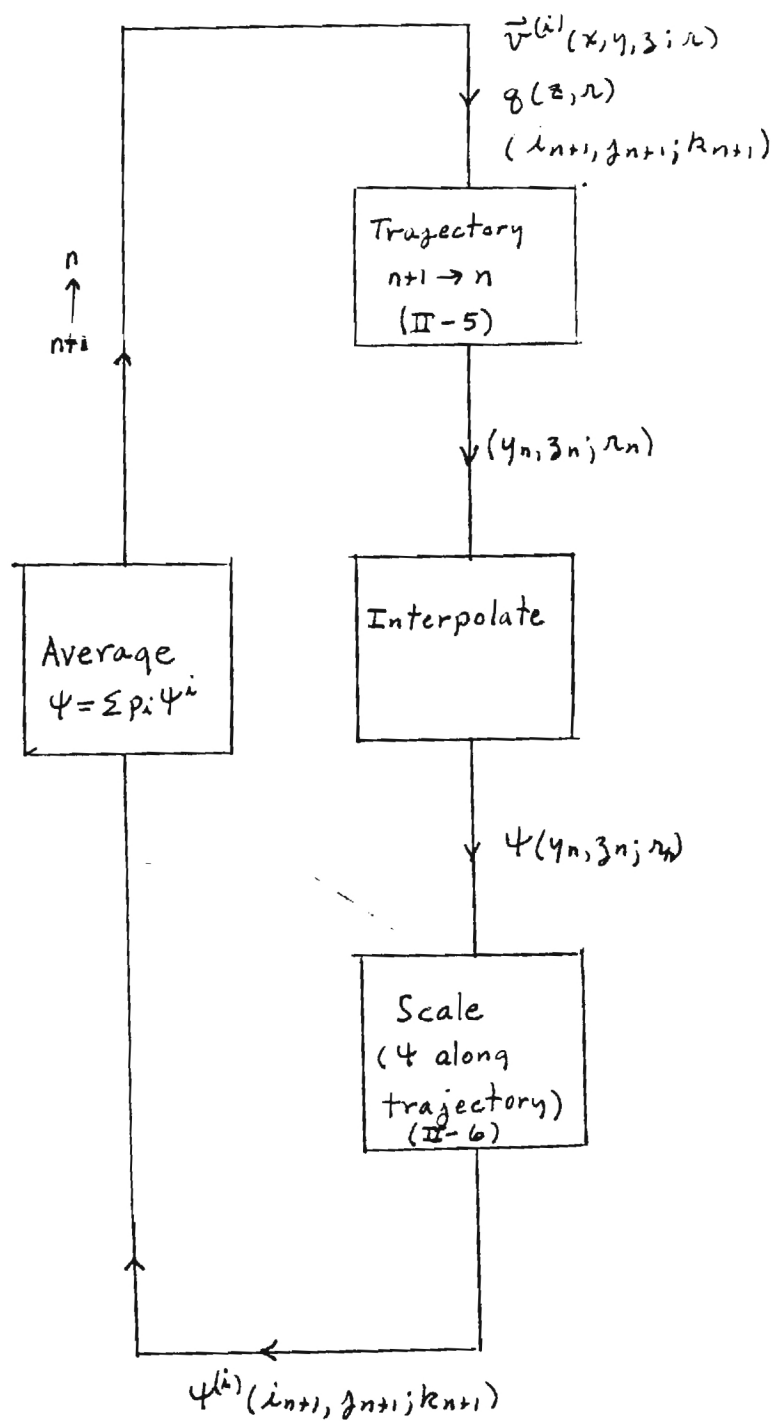
Step 4 involves the scaling of  $\Psi^{(i)}$  along the trajectory via (II-6). This requires knowledge of  $q(z,r)$  along the trajectory, again given in terms of an explicit formula coming from the bubble dynamic theory.

Step 5 involves the weighted average of the  $\Psi^{(i)}$  passed along each of the  $i$  trajectories, and this must be done for each of the  $(i_{n+1}, j_{n+1}; k_{n+1})$  lattice points.

Successive iteration of steps 1-5 allows one to establish the time evolution of the wake bubble density.



## B-2. Random Walk Program Block Diagram



## CONCLUSION

Experimentally based analytical relations relating white cap coverage and subsurface bubble densities to sea state have been extrapolated to infer an estimate on subsurface bubble densities in equilibrium with white water at 100% coverage. Consistent with the notion of a stability point in the growth-decay curve of the surface ship white water, an estimate at this stability point was made for the volumetric bubble density in the water immediately below the white water. This bubble current density was then found to lead to a air volume current from below nearly equal to the air volume current produced by bursting bubbles at the upper white water surface, as estimated from experiments on white water. Since the latter currents were also found to be compatible with observed white water lifetimes and thickness measurements one can consider that a self consistent view of a connection between white water growth and subsurface bubble currents exists and is applicable to surface ship bubble generation using observed lifetimes of surface ship white water wakes. The resulting densities and sea state distribution laws are compatible with those inferred from acoustic measurements.

It remains to give a relation between the subsurface bubble density scale and ship speed. These are supplied by relating  $\bar{\alpha}$  to observed white water length through surface ship white water scaling laws as given in Peltzer<sup>7</sup>, in particular

$$(I-28) \quad 1 - \frac{T_L n^{.32}}{(4.44 u_s^{1/2} - 5s)} < \bar{\alpha} < 1 - \frac{T_L n^{.32}}{(13.7 u_s^{1/2} - 5s)},$$

where  $n$  is the number of propeller revolutions per second. Hence one has an estimate, via (I-23) of the time average scale for the volumetric subsurface bubble density in the white water region.

The random walk description of bubble transport is straight forward. It involves the passing of data from one transverse (to the white water) data plane to another, with the bubble density on an initial data plane and with possible fluid flow fields and their probabilities as input.

## REFERENCES

1. J. Wu, "Oceanic Whitecaps and Sea State", J. Phys. Oceanography, 9, 1064-1068 (1979)
2. E. C. Monahan, "Oceanic Whitecaps", J. Physical Oceanography, 1, 139-144 (1971)
3. Y. Toba and M. Chaen, "Quantitative Expression of the Breaking of Wind Waves on the Sea Surface", Rec. Oceanographic Works Japan, 12, 1-11 (1973)
4. J. Wu, "Bubble Populations and Spectra in Near-Surface Ocean: Summary and Review of Field Measurements", J. Geophysical Res., 88, C1, 457-463 (1981)
5. D. A. Kolovayev, "Investigation of the Concentration and Statistical Size Distribution of Wind-Produced Bubbles in the Near-Surface Ocean", Oceanology, Eng. Trans., 15, 659-661 (1976)
6. B. D. Johnson and R. C. Cooke, "Bubble Populations and Spectra in Coastal Waters: A Photographic Approach", J. Geophysical Res., 84, 3761-3766 (1979)
7. R. D. Peltzer, "White Water Wake Characteristics of Surface Vessels", NRL Memorandum Report 5335, June 5, 1984
8. Q. A. Zheng, V. Klemas, and Y.-H.L. Hsu, "Laboratory Measurements of Surface Bubble Lifetime", J. Geophysical Res., 88, C1, 701-706 (1983)
9. M. Struthwolf and D. C. Blanchard, "The Residence Time of Air Bubbles (400 microns Diameter at the Surface of Distilled Water and Sea Water", Tellus, 36B, 294-299 (1984)
10. S. Burger and D. C. Blanchard, "The Persistence of Air Bubbles at a Seawater Surface", J. Geophysical Research, 88, C12, 7724-7726 (1983)
11. J. Podzimek, "Size Spectra of Bubbles in the Foam Patches and of Sea Salt Nuclei in the Surf Zone, Tellus, 36B, 192-202 (1984)
12. S. Baldy and M. Bourguel, "Measurements of Bubbles in a Stationary Field of Breaking Waves by a Laser-Based Single Particle Scattering Technique", J. Geophysical Res., 90, C1, 1037-1047 (1985)
13. R. Wildt, Ed., "Physics of Sound in the Sea," Pt. IV, Gordon and Breach, New York, N.Y. (1968)
14. Y. Miyake and T. Abe, "A Study on the Foaming of Sea Water, Pt. I", J. of Marine Research, 7, #2, 67-73 (1948)
15. S. A. Thorpe, "A Model for the Turbulent Diffusion of Bubbles below the Sea Surface", J. of Physical Oceanography, 14, 841-854 (1984)
16. G. A. Garrettson, "Bubble Transport Theory with Application to the Upper Ocean", J. Fl. Mech., 59, 187-206 (1973)

FIGURE I  
UNIVERSAL WHITE WATER DISTRIBUTION  
(probability)

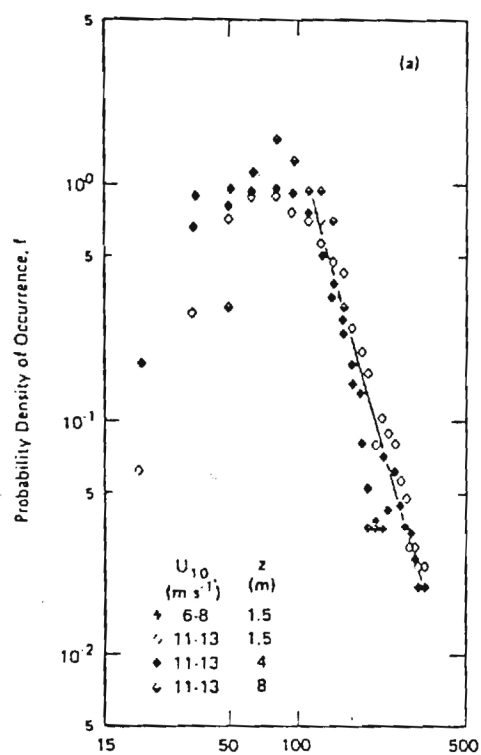


FIGURE II  
BUBBLE SURFACE LIFETIMES

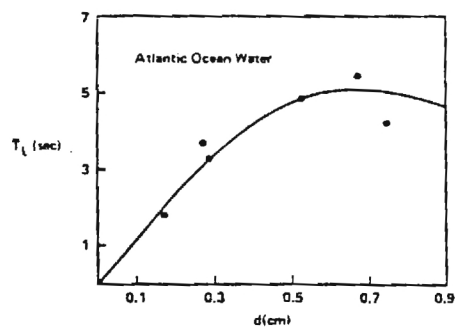


FIGURE III  
WAKE CENTERED COORDINATE SYSTEM

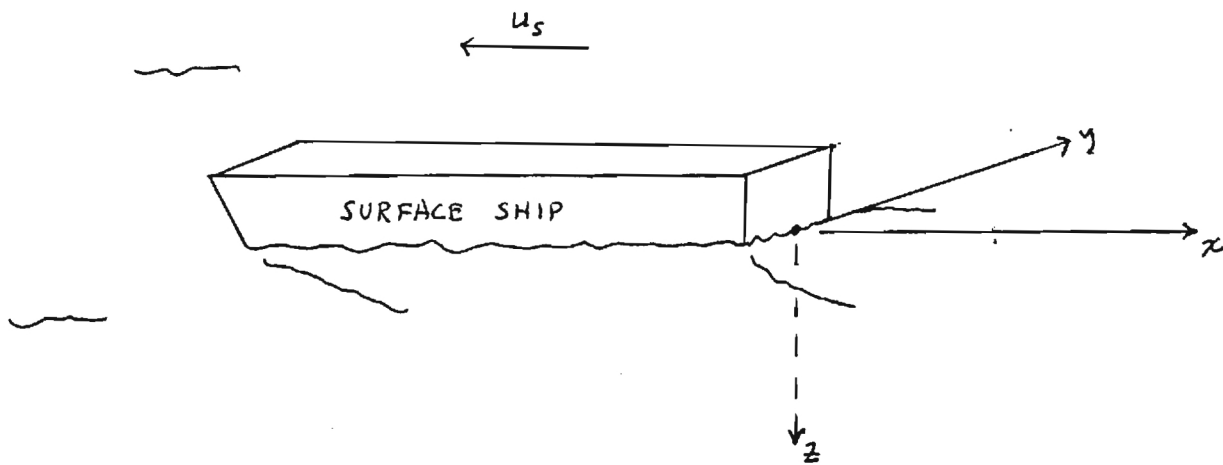


FIGURE IV  
RANDOM WALK DATA PLANES AND TRANSPORT

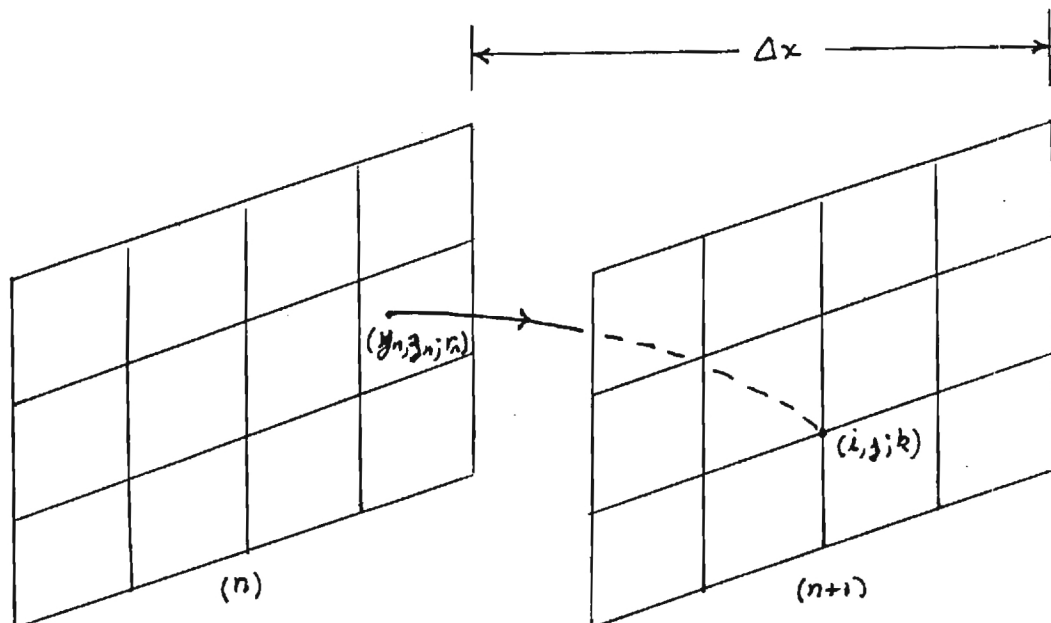


TABLE  
WHITE WATER SURFACE BUBBLE CHARACTERISTICS

Patch Status	$\bar{n}$ (#/cm <sup>2</sup> )	$\bar{r}$ (cm)	$\theta$ (cm)	$V_L/V_a$
initial $t < 5$ sec	23.22	.06	.03	.79
mature $5 < t < 10$	21.17	.081	.02	.30
decaying $10 < t < 30$	6.00	.20	.045	.33